Separation and Purification Technology 300 (2022) 121812

Contents lists available at ScienceDirect

Separation and Purification Technology

journal homepage: www.elsevier.com/locate/seppur

A hindered settling velocity model related to the fractal dimension and activated sludge flocs characteristics: Application to a sludge with a previous fragmentation and flocculation process

E. Asensi [a,*], E. Alemany [b]

[a] Institut Universitari d'Investigació d'Enginyeria de l'Aigua i Medi Ambient – IIAMA, Universitat Politècnica de València, Camí de Vera s/n, 46022 València, Spain
[b] Departamento de Matemática Aplicada, Universitat Politècnica de València, Camí de Vera s/n, 46022 València, Spain

ARTICLE INFO

Keywords:
Hindered settling
Settling velocity model
Fractal dimension
Activated sludge
Secondary settling tank

ABSTRACT

The modelling of the activated sludge hindered settling velocity as a function of the flocs characteristics and the incorporation of these models to the secondary settling tanks simulation is a hardly studied subject. Commonly used empirical models cannot describe the changes in the settling velocity caused by changes in the flocs characteristics. In this paper, a model for the hindered settling velocity as a function of the fractal dimension and other flocs characteristics is proposed. The model was used to describe the settling velocity after a flocculation process originated by activated sludge fragmentation. The model reproduces the observed abrupt decrease of hindered settling velocity in a small range of suspended solids concentration. It also enables to relate the flocs characteristics and the settling velocity to the fragmentation and sludge aggregation mechanisms.

1. Introduction

The activated sludge process is one of the most widely used biological treatments for organic matter and nutrients removal in a wastewater treatment plant (WWTP). The secondary settling tank plays an important role in this process, since it allows to obtain a clarified effluent, to thicken the sludge and store it during the peak flows.

The design and operation methods, and the models used to simulate the secondary settling tank based on solid flux theory, need information about the sludge hindered settling velocity (V_S) as a function of the suspended solids concentration (X) [1,2].

There are several hindered settling velocity models for activated sludge [1], but the most used are the exponential model ($V_S = k{\cdot}exp(-n_1{\cdot}X)$) and the power model ($V_S = k{\cdot}X^{-n1}$). Takács double exponential model ($V_S = k{\cdot}(\exp(-n_1{\cdot}(X - X_{min}) - \exp(-n_2{\cdot}(X - X_{min}))$, where X_{min} represents the non-settleable solids concentration, is also widely used since it allows to introduce hindered and discrete sedimentation into the secondary settler one-dimensional models [3]. To a lesser extent, the models proposed by Cho et al. [4] ($V_S = k{\cdot}exp(-n_1{\cdot}X)/X$, $V_S = k{\cdot}(1 - n_1{\cdot}X)^4{\cdot}exp(-n_2{\cdot}X)/X$ and $V_S = k{\cdot}(1 - n_1{\cdot}X)^4/X$), some polynomial models and other variants of the exponential and power models [1,2] have also been used. The parameters of these models (k, n_1 and n_2) do not need to have a physical meaning and they are determined experimentally.

Knowing the hindered settling velocity is also important since it allows calculating the settling velocity in the compression region from the expression: $V_C = V_S{\cdot}(1 - \rho_s/(g{\cdot}X{\cdot}(\rho_s - \rho)){\cdot}d\sigma/dX{\cdot}dX/dz)$, being ρ_s the dry sludge density, ρ the fluid density, $d\sigma/dX$ the effective solid stress gradient and dX/dz the concentration gradient [5,6].

Models for hindered settling velocity based on a balance of forces have also been developed. In some models, the hydrodynamic drag force is calculated considering that the flow in a suspension is equivalent to the flow through a porous media [4,7], whereas in other models a hindered settling factor is considered [8].

Kinnear [7] proposed the following equation using Darcy's law to calculate the hindered settling velocity taking into consideration the drag force: $V_S(\varepsilon) = (\rho_f - \rho){\cdot}g{\cdot}\varepsilon^3/(5{\cdot}S_0^2(1-\varepsilon){\cdot}\mu)$, being $\varepsilon = 1 - ((\rho_s - \rho)/(\rho_f - \rho)){\cdot}X/\rho_s$ the suspension porosity, μ the fluid viscosity, ρ_f the flocs density and S_0 the specific surface area of the primary particles. Kinnear [7] used this model to describe the activated sludge hindered settling velocity.

The model proposed by Richardson and Zaki [8], extended to suspensions, is expressed as $V_S(\varepsilon) = V_0{\cdot}\varepsilon^n$, being V_0 the flocs terminal settling velocity, ε the suspension porosity and n an exponent which depends in general on Reynolds number. The model is related to the fluid characteristics and to the flocs size and density through V_0. Richardson and Zaki model, and other variations of this model, have

* Corresponding author.
E-mail addresses: easensi@hma.upv.es (E. Asensi), ealemany@mat.upv.es (E. Alemany).

https://doi.org/10.1016/j.seppur.2022.121812
Received 1 June 2022; Received in revised form 14 July 2022; Accepted 23 July 2022
Available online 29 July 2022

Nomenclature

X	Suspended solids concentration
X_0	Initial X value for the settling test
$h(t)$	Settling curve
H_0	Initial h value for the settling test
V_S	Hindered settling velocity
V_{Si}	Initial hindered settling velocity
V_{Sf}	Final hindered settling velocity
V_0	Flocs terminal settling velocity
ρ_s	Dry sludge density
ρ_p	Primary flocs density
ρ_f	Flocs density
ρ	Fluid density
μ	Fluid viscosity
d_p	Equivalent primary flocs diameter
v_p	Primary flocs volume: $v_p = \frac{\pi}{6} \cdot d_p^3$
d_f	Equivalent flocs diameter
v_f	Flocs volume: $v_f = \frac{\pi}{6} \cdot d_f^3$
v_s	Solids volume contained within the floc
D_f	Flocs fractal dimension
c	Packing coefficient
N	Number of primary flocs that form the flocs: $N = c \cdot \left(\frac{d_f}{d_p}\right)^{D_f}$
ε_f	Flocs porosity: $\varepsilon_f = \frac{v_f - v_s}{v_f}$
ε_{fp}	Flocs porosity due to the primary flocs: $\varepsilon_{fp} = \frac{v_f - N \cdot v_p}{v_f}$
n_f	Number of flocs per unit volume
Re	Reynolds number: $Re = \frac{\rho \cdot d_f \cdot V_0}{\mu}$
j	Aggregate volume index: $j = \frac{v_f}{v_s}$
ϕ_f	Flocs volumetric fraction: $\phi_f = \frac{j \cdot X}{\rho_s}$
n	Richardson and Zaki exponent: $V_S = V_0 \cdot \left(1 - \frac{j}{\rho_s} \cdot X\right)^n$

been widely used to describe the hindered settling velocity for several suspension types [9–12] and for the activated sludge too [13–15].

V_S models traditionally used in wastewater treatment, are empirical or semi-empirical formulas whose parameters are adjusted experimentally by sedimentation tests. These hindered settling velocity models only depend on X, thus they cannot describe changes in the sludge sedimentability due to changes in the fluid or sludge characteristics. However, several studies have shown that the activated sludge settling velocity depends on the flocs density, size and fractal dimension [16–19]. These flocs characteristics vary seasonally in urban WWTPs [20,21], and they are also modified by the presence of coagulants and by the flocs breakage and flocculation processes [19,22].

Several authors have described the existence of a sludge acceleration process in the hindered settling test performed with industrial wastewater plants activated sludge [13,15], with primary sludge coagulated with an anionic organic polymer [23] and with colloidal suspensions with weak gel structure [24].

Asensi et al. [15] explained the observed activated sludge acceleration process considering physical–chemical mechanisms that generate sludge fragmentation and flocculation. The authors used Richardson and Zaki model to characterize sludge sedimentability and to estimate the suspended solid concentration where the sudden descent of the hindered settling velocity reached after the acceleration process is observed. Nevertheless, the model used to describe this steep descent has the inconvenience of introducing a discontinuity in $V_S(X)$.

The modelling of the activated sludge hindered settling velocity as a function of the flocs characteristics and the incorporation of these models to the secondary settling tanks simulation is a subject hardly studied. In this paper, a model for the activated sludge hindered settling velocity given as a function of the flocs fractal dimension and other sludge characteristics is proposed. The aim of the performed study is to use this model to describe the hindered settling velocity after a flocculation process originated by activated sludge fragmentation. The novelty of the model lies in being able to describe the observed sudden decrease of the settling velocity in the settling test and characterize the structure of the flocs formed from the primary flocs during the sludge acceleration phase.

2. Materials and methods

The industrial WWTP Ford Spain located in Almussafes, Valencia (Spain) provided the activated sludge samples that were used to perform the tests supporting these studies. The plant performs a set of physical–chemical treatments followed by a biological treatment with an oxidation ditch. The physical–chemical treatments make use of Ca $(OH)_2$, iron and aluminium salts, and polymers. In this paper, experimental results of a previous study performed by Asensi et al. [15] are used.

2.1. Settling tests

Settling tests were performed using two cylindrical columns (1.1 m height and 0.12 m of diameter) following the methodology described by Asensi et al. [15]. The rapid sludge stirring performed before the settling tests was meant to eliminate the memory effect of the sludge [13,15] and to reproduce the hydrodynamic conditions the sludge is subjected to at the treatment plant, before entering the settling tank. The sludge suspended solids concentration (X) was determined using the Standard Method 2540 D [25].

2.2. Hindered settling velocity calculation

Activated sludge hindered settling velocity (V_S) is usually determined from a settling test as the slope of the settling curve ($h(t)$) at the "straight zone" of the hindered settling zone. In this zone (zone "a" in Fig. 1), X stays constant and equal to the test initial suspended solids concentration (X_0). The relation V_S (X) is obtained with the traditional method, performing settling tests with different X_0 concentrations [26].

In a settling test, besides the information given by the traditional method at the hindered settling zone, it is also possible to calculate $V_S(X)$ in the transition zone. Kynch's graphical method allows obtaining V_S and X for values of X larger than the solid concentration at the inflection point of the flux function given by $f(X) = X \cdot Vs(X)$ [27].

The zones described by Lester et al. [28] in the settling mode 3 (Fig. 1) can be identified in the activated sludge settling tests. In the transition zone "b", where the characteristic lines (lines of constant X and constant settling velocity) arise from the bottom of the vessel, Vs can be determined as a function of X by means of Eq. (1) [29]. The solids concentration that separates the transition zones "b" and "c" in Fig. 1b (X_{max}), represents the highest concentration for which it is possible to calculate V_S and X using Kynch's graphical method [9,28].

$$V_S(X) = h'(t) = -\frac{dh(t)}{dt}$$
$$X = \frac{X_0 \cdot H_0}{h(t) - t \cdot h'(t)} \quad (1)$$

This method can be applied in activated sludge suspensions since it was observed the existence of characteristic lines in the settling tests performed with this type of sludge [30]. However, applying this method presents the difficulty of determining experimentally the point "X_{max}" in Fig. 1b that delimits zone "b" in the activated sludge test. Betancourt et al. [31] used a method based in Eq. (1) to determine the solids flow function (from which $V_S(X)$ can be obtained) for activated sludge. However, they did not check that the experimental data used did not

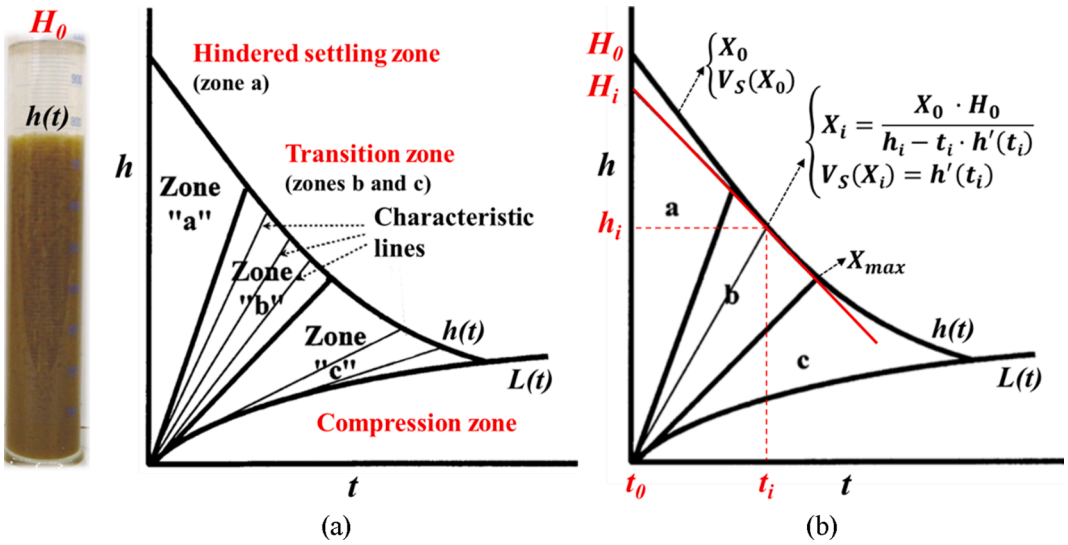

Fig. 1. Batch settling test (adapted from [9]) (a) Classification of zones in a settling test. (b) Calculation of X_i and $V_S(X_i)$ at instant t_i of the transition zone "b".

belong to the transition zone "c" or to the compression zone, where Kynch's method does not work correctly.

To avoid the method difficulties to determine V_S and X in the activated sludge settling test in the transition zone, the following procedure was applied:

- Settling tests are performed with different initial suspended solids concentrations (X_0).
- V_S in zone "a" (Fig. 1) is determined from the settling tests using the traditional method [26].
- $V_S(X)$ model that best describes the experimental results is obtained and the related linear model is considered. For the sludge under study, Asensi et al. [15] showed that the best model was that of Richardson and Zaki, thus, the linear model $V_S^{1/n} = k - m \cdot X$ was used.
- The following steps to determine X_i and $V_S(X_i)$ for each settling test in the transition zone are carried out:
  1. The settling velocity $V_S(X_i) = h'(t_i) = (-dh/dt)_i$ at each experimental point of the transition zone $\{t_i, h_i\}$ is determined numerically as the slope of the line fitted through that point, the previous point $\{t_{i-1}, h_{i-1}\}$ and the following point $\{t_{i+1}, h_{i+1}\}$.
  2. The suspended solids concentration is determined at each point as $X_i = X_0 \cdot H_0 / H_i$, where H_0 is the initial height interface and H_i ($H_i = h_i - t_i \cdot h'(t_i)$) is the intersection between the tangent to the curve h (t) at t_i and the vertical axis (Fig. 1b, Eq. (1)).
  3. V_S versus X is graphically represented according to the linear relationship of the considered model. For the Richardson and Zaki model, the points $\{X_i, h'(t_i)^{1/n}\}$ are represented together with the point obtained in zone "a" of the settling test $\{X_0, V_S^{1/n}\}$.
  4. A linear regression and analysis of randomness of normalized residuals is performed. If the distribution of residuals is not random the point in the tail of largest X is removed.
  5. Go back to point 3 until a situation of randomness of residuals is reached.

The procedure described above was performed by programming the corresponding algorithm in Mathematica (Wolfram®). The analysis of point 3 can also be made without linearizing $V_S(X)$ by making nonlinear regressions. The same results were obtained making linear and nonlinear regressions. Fig. 2 shows a settling test example with the results obtained for the first and last iteration. It can be observed that initially the normalized residuals are not random (Fig. 2a), and finally, after eliminating iteratively the points in the queue with larger X, a good fit with randomly distributed residuals is obtained (Fig. 2b).

The proposed method assumes that the relation $V_S(X)$ is the same in zones "a" and "b" (Fig. 1), since in both zones hindered sedimentability occurs and the same sludge characteristics are encountered. Therefore, points that belong to zone "b" $\{X_i, h'(t_i)^{1/n}\}$ together with those of zone "a" $\{X_0, V_S^{1/n}\}$, will fit to a line. The rest of points will deviate from the line, because the X_i calculation made with equation $X_i = X_0 \cdot H_0 / H_i$ in zone "c" is not correct or because the points are located at the compression zone.

It is important to highlight that the aim of this method is not to determine the solids flow function, or the model describing best $V_S(X)$ for a given sludge. Once known a $V_S(X)$ model that correctly describes the sludge sedimentation, the focus is on determining the parameters of the model using the additional information provided by the transition zone in the settling test.

2.3. Flocs characteristics

Sludge samples were obtained from the settling column during the stirring process performed at the beginning. The flocs of this initial sludge agitation stage are known as primary flocs.

Dry sludge density (ρ_s) was calculated using a pyknometer method [32] and the primary flocs density (ρ_p) was obtained by a method that uses centrifugation in homogenous density solutions [33].

Image analysis techniques were used to measure the primary flocs equivalent diameter (d_p), defined as the diameter of a circle with the same projected surface of the floc. Images were obtained using a Hund Wetzlar H500 microscope with a 10 megapixels digital camera. Image processing and analysis was performed using the methodology described by Asensi et al. [19] and using the MATLAB program (MathWorks®) developed by these authors. An equivalent diameter of 3.5 μm was set to eliminate debris.

2.4. Linear and nonlinear regressions

The linear and nonlinear regressions of the models under study and the implementation of the described algorithm for the calculation of V_S and X in the transition zone, were performed with the program Mathematica (Wolfram®). To compare the models, the goodness of fit was established using the Sum of Squares Residuals (SSR) and the coefficient of determination from nonlinear regressions (R^2). The parameters of the models were determined to be significant if p-value < 0.05. A runs test was performed to determine the randomness of the residuals.

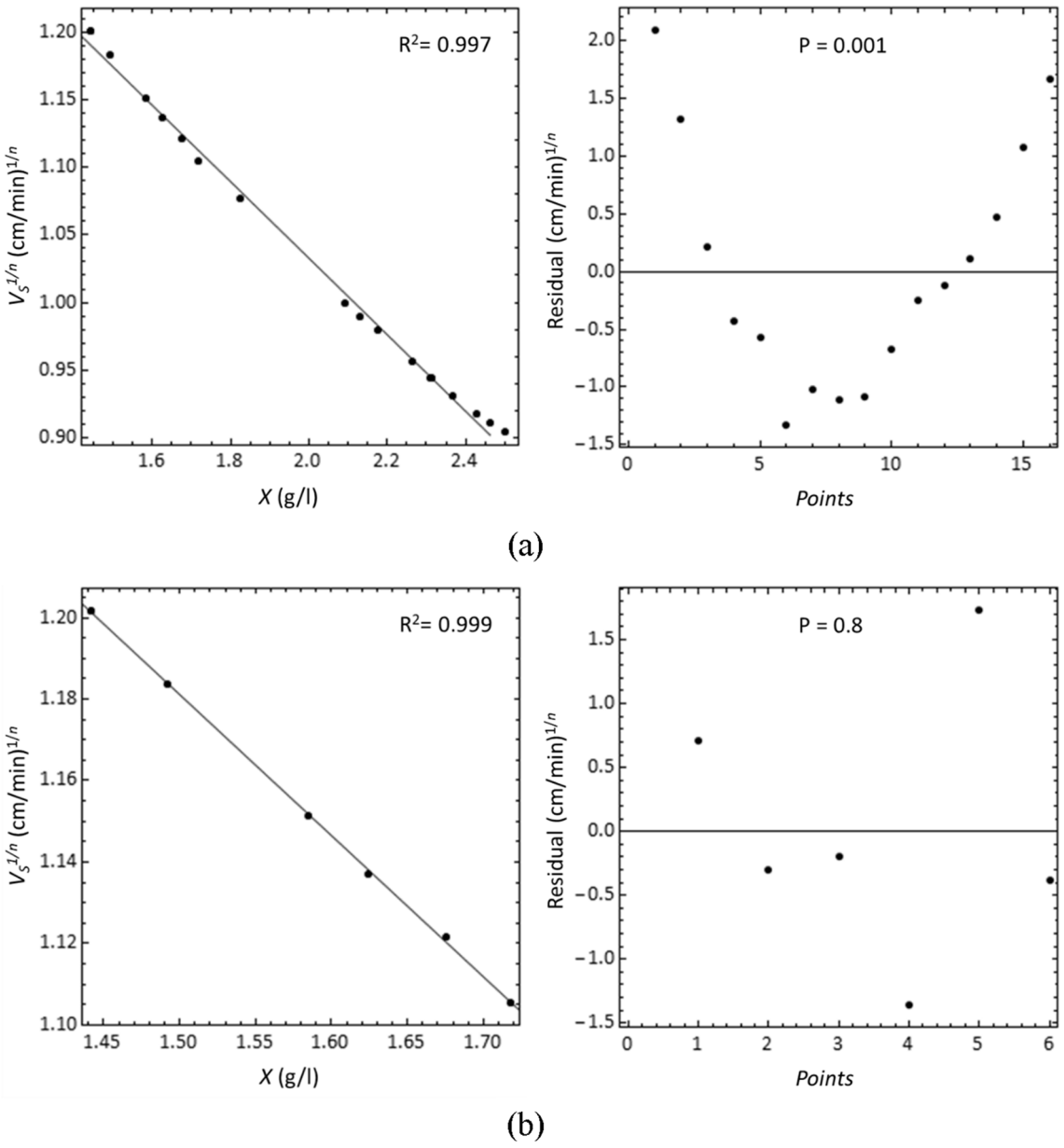

Fig. 2. Fitting of the settling velocity in the transition zone. (a) Initial adjustment. (b) Final adjustment. P: probability of the residuals being randomly distributed, obtained using the runs test.

3. Results and discussion

3.1. Characterization of activated sludge

The results obtained for the dry sludge density (ρ_s) was 1.71 ± 0.04 g/ml, and for the primary flocs density (ρ_p), 1.046 ± 0.004 g/ml. The densities are higher than typical values observed for urban WWTPs. This is due to the flocs adsorption of the inert colloidal particles, precipitates, polymers and coagulant residues escaping from the physical–chemical process.

Experimental data for the flocs equivalent diameter fitted a lognormal distribution. Since the lognormal distribution is not symmetric, the median was used as a central measure for the primary flocs diameter (d_p). A d_p value of 9.7 μm was obtained and 85% of the flocs were found to be smaller than 25 μm. The small size of the primary flocs is typical of the pin-point flocs, which are characteristic of the extended aeration biological processes.

3.2. Setting tests results

Results obtained in the settling tests are shown in Fig. 3a. In all settling tests two stages with constant hindered settling velocity were observed. It was also observed in the tests: an initial stage (1) with constant initial settling velocity V_{Si}, a later stage where the sludge is accelerated and the settling rate increases (2), a stage (3) in which the final constant settling velocity V_{Sf} is reached and a final stage (4) where the settling velocity decreases. These stages just described also appeared in the tests performed without initial rapid stirring of the sludge. The sludge acceleration process starts a few minutes or several hours after the beginning of the test, depending on the value of the suspended solids concentration. Chen et al. [13] also described the existence of two stages with constant hindered settling velocity in the activated sludge settling test, and an intermediate acceleration stage. And so did Zhao [23], in the tests with primary sludge coagulated with an aluminium salt and an anionic polymer.

Fig. 3b shows the V_{Sf} obtained as a function of X in the final hindered

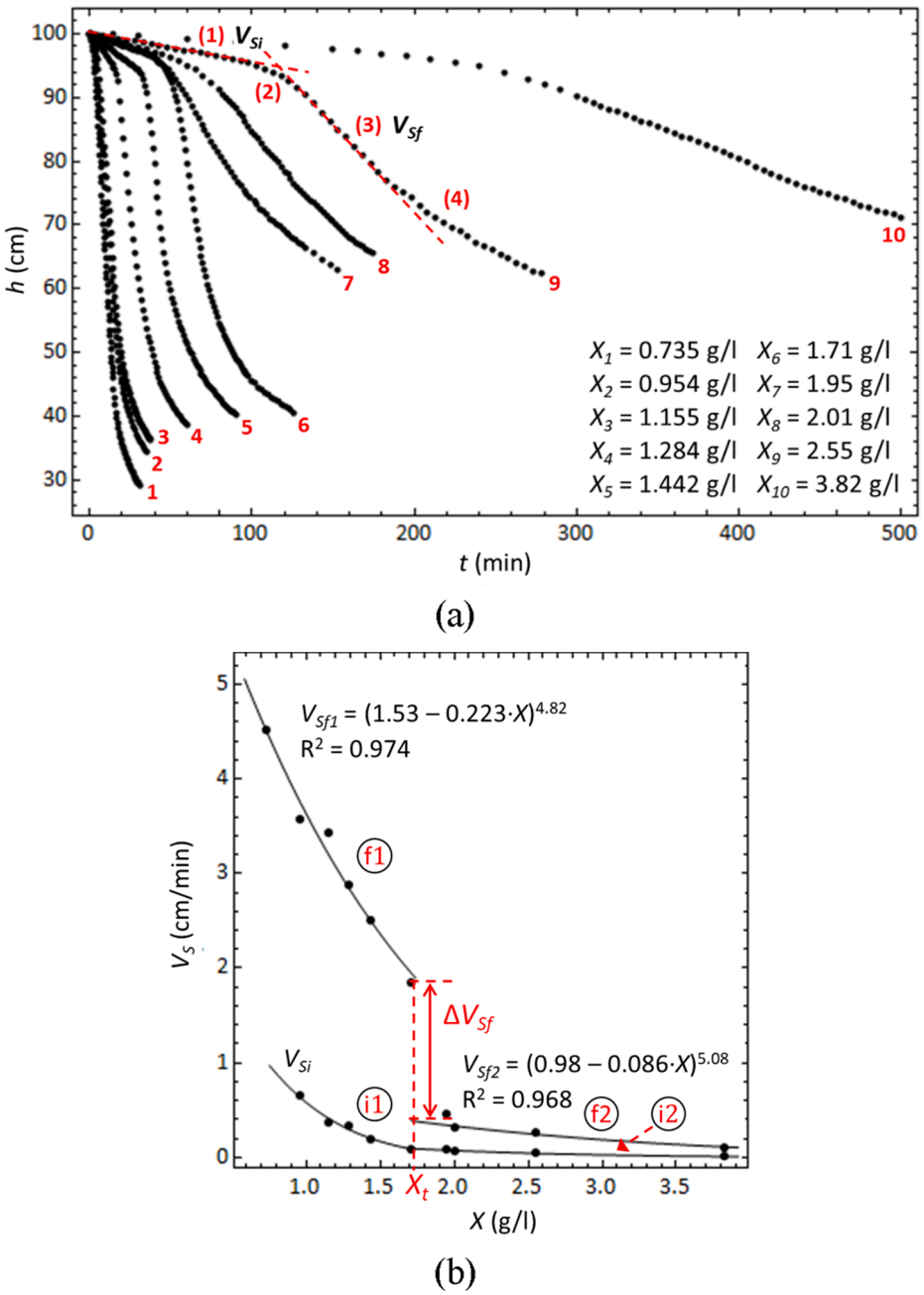

Fig. 3. (a) Settling curves h(t) from the tests performed in the experiments. (b) Initial (V_{Si}) and final (V_{Sf}) hindered settling velocity obtained from the settling tests as a function of X.

settling stage. An abrupt decrease of V_{Sf} in a small X interval is observed. This abrupt decrease of the hindered settling velocity is not normally observed in the activated sludge settling tests.

From the experimental results two zones can be highlighted in Fig. 3b: a zone "f1" for low X concentrations ($X < X_t$) where V_{Sf} decreases with increasing X, until the zone where V_{Sf} sharply decreases. And a later zone "f2" where V_{Sf} decreases again uniformly.

Asensi et al. [15] used the model proposed by Font et al. [9] to characterize $V_S(X)$ and estimate the concentration X where the sudden drop in settling velocity occurs. However, this model cannot describe the sudden drop in V_{Sf}.

3.3. Description of the hindered settling model as a function of the flocs fractal dimension

The usual models for the activated sludge hindered settling velocity do not allow to describe the sharp decrease in $V_{Sf}(X)$ observed in Fig. 3b. To study and describe this observed sudden decrease in the hindered settling velocity, it was first considered the model used by Font et al. [9] for metal hydroxide suspensions and by Asensi et al. [15] for activated sludge (Eq. (2) and (3)).

$$V_S = V_0 \cdot \left(1 - \frac{j}{\rho_s} \cdot X\right)^n \quad (a)$$

$$\begin{cases} \dfrac{5.09 - n}{n - 2.73} = 0.104 \cdot Re^{0.877} \qquad Re < 500, \quad \phi_f > 1 & (b) \\ V_0 = \dfrac{g \cdot (\rho_f - \rho) \cdot d_f^2}{18 \cdot \mu} \cdot \dfrac{1}{1 + 0.15 \cdot Re^{0.687}} & (c) \\ Re = \dfrac{\rho \cdot d_f \cdot V_0}{\mu} & (d) \end{cases} \quad (2)$$

$$\rho_f = \frac{\rho_s + (j-1) \cdot \rho}{j} \quad (3)$$

In this model, the flocs diameter (d_f) represents the equivalent diameter of a sphere with the same volume of the floc and the flocs density (ρ_f) is calculated by mass balance with Eq. (3). V_0 is the flocs terminal settling velocity for Reynolds numbers (Re) smaller than 500. The aggregate volume index (j) is defined as the quotient between the volume of the flocs (v_f) and the volume of the solids contained within the flocs (v_s). This parameter is related to the density of the floc by Eq. (3) and can also be related to the total porosity of the floc (ε_f) as: $\varepsilon_f = (v_f - v_s)/v_f = 1 - 1/j$. An increase of j in the floc implies a decrease in ρ_f and an increase in ε_f due to the increase in the water content of the floc. The model exponent (n) calculation is valid for flocs volumetric fractions ($\phi_f = j \cdot X/\rho_s$) greater than 1. The flocs volumetric fraction represents the total volume occupied by the flocs with respect to the total volume of the suspension.

Activated sludge flocs have a fractal structure, since the flocs are statistically self-similar and have properties such as mass, area, perimeter, etc. that can be characterized by means of a fractal dimension [16,19,22,34,35]. The flocs fractal dimension (D_f) allows to calculate the number of primary particles or primary flocs (generators) that form the flocs as $N = c \cdot (d_f/d_p)^{Df}$ [36], being d_f the floc equivalent diameter ($v_f = \pi \cdot {d_f}^3/6$), d_p the generators equivalent diameter ($v_p = \pi \cdot {d_p}^3/6$) and c the packing coefficient. It is usually considered c = 1 [37]. Calculating the floc mass as the sum of the primary flocs mass and the mass of the water contained inside the floc ($v_f \cdot \rho_f = N \cdot v_p \cdot \rho_p + (v_f - N \cdot v_p) \cdot \rho$), and considering the fractal N relation, Eq. (4) is obtained. Eq. (4) allows to calculate the flocs density (ρ_f) as a function of the flocs diameter (d_f), the fractal dimension (D_f) and the characteristics of their primary flocs (ρ_p and d_p). In the same way, a fractal relation with the same fractal dimension D_f can be obtained for the mass of flocs.

$$\rho_f - \rho = (\rho_p - \rho) \cdot \left(\frac{d_f}{d_p}\right)^{D_f - 3} \quad (4)$$

Considering that the flocs density is related to the aggregate volumetric index as shown by Eq. (3), Eq. (4) leads to an expression relating j to d_f through the fractal dimension (Eq. (5)).

$$j = \frac{\rho_s - \rho}{\rho_p - \rho} \cdot \left(\frac{d_f}{d_p}\right)^{3 - D_f} \quad (5)$$

Finally, the hindered settling velocity can be written as a function of the fractal dimension and other flocs characteristics by means of Eq. (6).

$$V_S = V_0 \cdot \left(1 - \frac{\rho_s - \rho}{\rho_s \cdot (\rho_p - \rho)} \cdot \left(\frac{d_f}{d_p}\right)^{3 - D_f} \cdot X\right)^n \quad (a)$$

$$\begin{cases} \dfrac{5.09 - n}{n - 2.73} = 0.104 \cdot Re^{0.877} \qquad Re < 500, \quad \phi_f > 1 & (b) \\ V_0 = \dfrac{g \cdot (\rho_p - \rho) \cdot d_p^{3 - D_f}}{18 \cdot \mu} \cdot \dfrac{d_f^{D_f - 1}}{1 + 0.15 \cdot Re^{0.687}} & (c) \\ Re = \dfrac{\rho \cdot d_f \cdot V_0}{\mu} & (d) \end{cases} \quad (6)$$

The proposed model considers an ideal approximation to the activated sludge by means of an equivalent system formed by spherical and impermeable flocs. An equivalent diameter representative of the size distributions of flocs (d_f) and primary flocs (d_p) is used to characterize their size (Fig. 4). The introduction of the flocs fractal structure allows to relate the flocs density to their diameter and primary flocs characteristics. The model can be used considering a fractal structure made either of primary particles (single-particle-fractal model) or of primary flocs (cluster-fractal model) [36]. If the flocs are generated by primary particles, then $\rho_p = \rho_s$.

Eq. (6c) agrees with the equation proposed by Khelifa and Hill [38] for the fractal flocs terminal settling velocity considering that the flocs form factor is equal to one (spherical flocs) and that flocs are made of mono-sized primary particles. In Khelifa and Hill [38] equation d_p is the median of the primary particles size distribution.

Heath et al. [11] and Grabsch et al. [10] used a model based on Richardson and Zaki model to estimate the calcite fractal dimension from the settling tests. The model proposed by Heath et al. [11] and Lockwood et al. [12] agrees with Eq. (6) in the case of a laminar regime and $\rho_p = \rho_s$.

Eq. (7a) allows to estimate the flocs porosity (ε_f) and Eq. (7b) the flocs porosity due to the larger pores generated from the primary flocs (ε_{fp}), considering the solids volume contained within the floc (v_s), the primary flocs volume ($N \cdot v_p$) and the flocs volume (v_f).

$$\varepsilon_f = \frac{v_f - v_s}{v_f} = 1 - \frac{\rho_p - \rho}{\rho_s - \rho} \cdot \left(\frac{d_f}{d_p}\right)^{D_f - 3} \quad (a) \qquad (7)$$

$$\varepsilon_{fp} = \frac{v_f - N \cdot v_p}{v_f} = 1 - \left(\frac{d_f}{d_p}\right)^{D_f - 3} \quad (b)$$

Assuming that solids are all contained within the flocs, the average number of flocs per unit volume (n_f) is calculated as the ratio between the flocs volumetric fraction (ϕ_f) and the flocs average volume (v_f), the latter calculated from the equivalent diameter definition. To eliminate

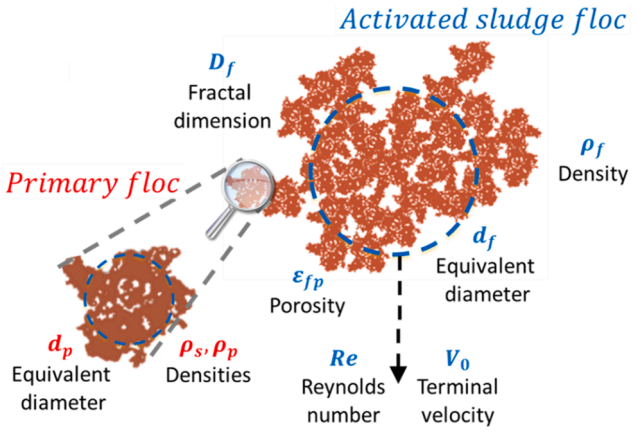

Fig. 4. Flocs characteristics used in the hindered settling model.

the effect of the increment in the flocs number due to the X increment, the average number of flocs per unit mass of X is estimated from Eq. (8).

$$\frac{n_f}{X} = \frac{6\cdot(\rho_s - \rho)}{\pi\cdot\rho_s\cdot(\rho_p - \rho)} \cdot \frac{d_p^{D_f-3}}{d_f^{D_f}} \tag{8}$$

The advantage of the proposed $V_S(X)$ model, compared to other activated sludge empirical models commonly used, is that it establishes a link between V_S and the flocs characteristics. The model allows introducing the fractal structure and other physical floc properties, as well as the characteristics of the primary flocs that form the flocs (Fig. 4). This is an important aspect since the model can be useful to model and connect the hindered settling process to other processes that could affect the flocs structure: seasonal changes in flocs or disruptions in the biological treatment, flocculation processes at the settling tank inlet, addition of coagulants or an inert compound to improve the sedimentability of the sludge, existence of previous physical–chemical treatments, decrease of the flocs density due to denitrification processes, etc.

In this study, the proposed model is used to describe the activated sludge final hindered settling velocity after the fragmentation of the initial sludge structure and the subsequent flocculation process taking place when the sludge is accelerated.

3.4. Application of the model in the final hindered settling velocity stage

To make the regressions for $V_S(X)$ and to obtain the parameters n, d_f and D_f of the model proposed in this article (Eq. 6), the iterative process described in Fig. 5 was used (see Appendix A). To that aim, the experimental results of the settling test where used (V_S and X) as well as the primary flocs characteristics (ρ_S, ρ_p and d_p).

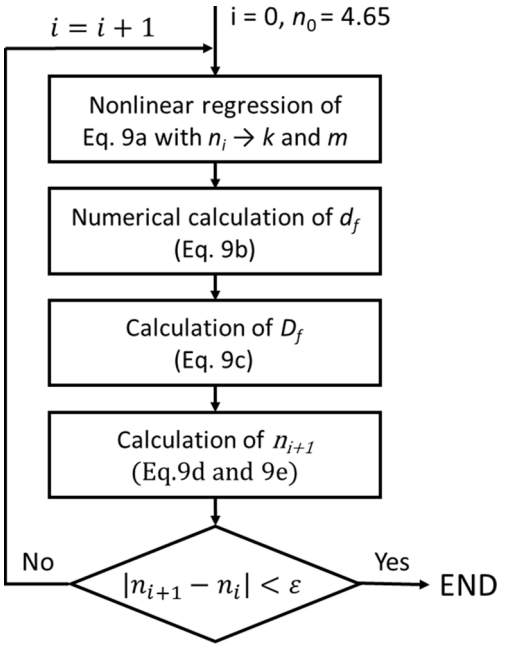

Fig. 5. Algorithm used in the regressions of $V_S(X)$ model (Eq. (6)).

$$V_S = (k - m\cdot X)^{n_i} \quad (a)$$

$$k^{n_i} + 0.15\cdot\left(\frac{\rho}{\mu}\right)^{0.687}\cdot k^{1.687\cdot n_i}\cdot d_f^{0.687} - \frac{g\cdot(\rho_S - \rho)}{18\cdot\mu\cdot\rho_S}\cdot\frac{k}{m}\cdot d_f^2 = 0 \quad (b)$$

$$D_f = \frac{3 - ln\left(\frac{m\cdot\rho_S}{k}\cdot\frac{\rho_p - \rho}{\rho_S - \rho}\right)}{ln\left(\frac{d_f}{d_p}\right)} \quad (c)$$

$$Re = \frac{\rho\cdot d_f\cdot k^{n_i}}{\mu} \quad (d)$$

$$n_{i+1} = \frac{5.09 + 2.73\cdot 0.104\cdot Re^{0.877}}{1 + 0.104\cdot Re^{0.877}} \quad (e) \tag{9}$$

Fig. 3b shows the results of the V_{Sf} (X) regression in the two zones separated by the observed sudden change. But using the model this way does not allow describing the sharp decrease in V_{Sf}.

3.4.1. Flocs characteristics in the final hindered settling stage

To study the sudden $V_{Sf}(X)$ descent, the settling velocity experimental results in the transition zone of the settling tests (Fig. 3a) were considered using the methodology described in Section 2.2. Fig. 6a shows that the V_{Sf} (X) values obtained experimentally in the transition zone do not follow the tendency of those obtained in the final hindered settling stage.

The methodology used is based on Kynch's theory and assumes that the selected points from the transition zone belong to zone "b" of Fig. 1a. Assuming a correct methodology, the observed differences in the settling tests (Fig. 6a) are due to differences in flocs characteristics from one test to the other due to the previous flocculation process taking place during the sludge acceleration phase. Assuming that this hypothesis is correct, the $V_S(X)$ proposed model allows to estimate the flocs characteristics after the sludge acceleration process. In each settling test, the d_f, j, D_f, V_0, n and Re values were obtained from the regressions carried out with Eq. (6), considering the transition and final hindered settling zones experimental data (Fig. 6a).

The flocs diameter and the aggregate's volumetric index decrease with increasing X concentration (Fig. 6b and c), while the flocs fractal dimension in zones f1 and f2 increases until reaching a maximum value and then decreases (Fig. 6d). In the zone where an abrupt decrease in V_{Sf} is observed, a smooth transition in d_f, a sharp increase in j and a sharp decrease in D_f occurs.

Flocs in zone f1 have an equivalent diameter between 3.2 and 0.9 mm, and in zone f2 a size smaller than 0.65 mm. These results are compatible with the settling tests observations where large flocs were encounter in zone f1 of some settling tests. Chen et al. [13] also observed the formation of large flocs in the final settling stage for low X concentrations, starting from a homogeneous sludge.

The flocs fractal dimension varies between 2.27 and 2.39 (Fig. 6d). These values are compatible with the experimental results obtained for the activated sludge flocs fractal dimension in other studies: 1.96–2.44 [16,34].

It was determined that the best model to describe d_f (X) was a linear model (Eq. (10a)) and for j (X) an exponential model (Eq. (10b)), since these models provided high R^2 values and the lowest SSR values (see Appendix B). Fig. 6b and c show the regression results of these models.

$$d_f = d_{f0} - k_f\cdot X \quad (a)$$

$$j = j_0\cdot e^{-k_j\cdot X} \quad (b) \tag{10}$$

If we assume the hypothesis that the primary particles forming the flocs after the acceleration process are the primary flocs, Eq. (5) allows to calculate $D_f(X)$ from Eq. (10) leading to Eq. (11). Fig. 6d shows that Eq. (11) correctly describes the variation in the fractal dimension as well as the sharp D_f decrease when passing from zone f1 to zone f2, from the experimental results obtained in zone f1. That way, the flocs fractal

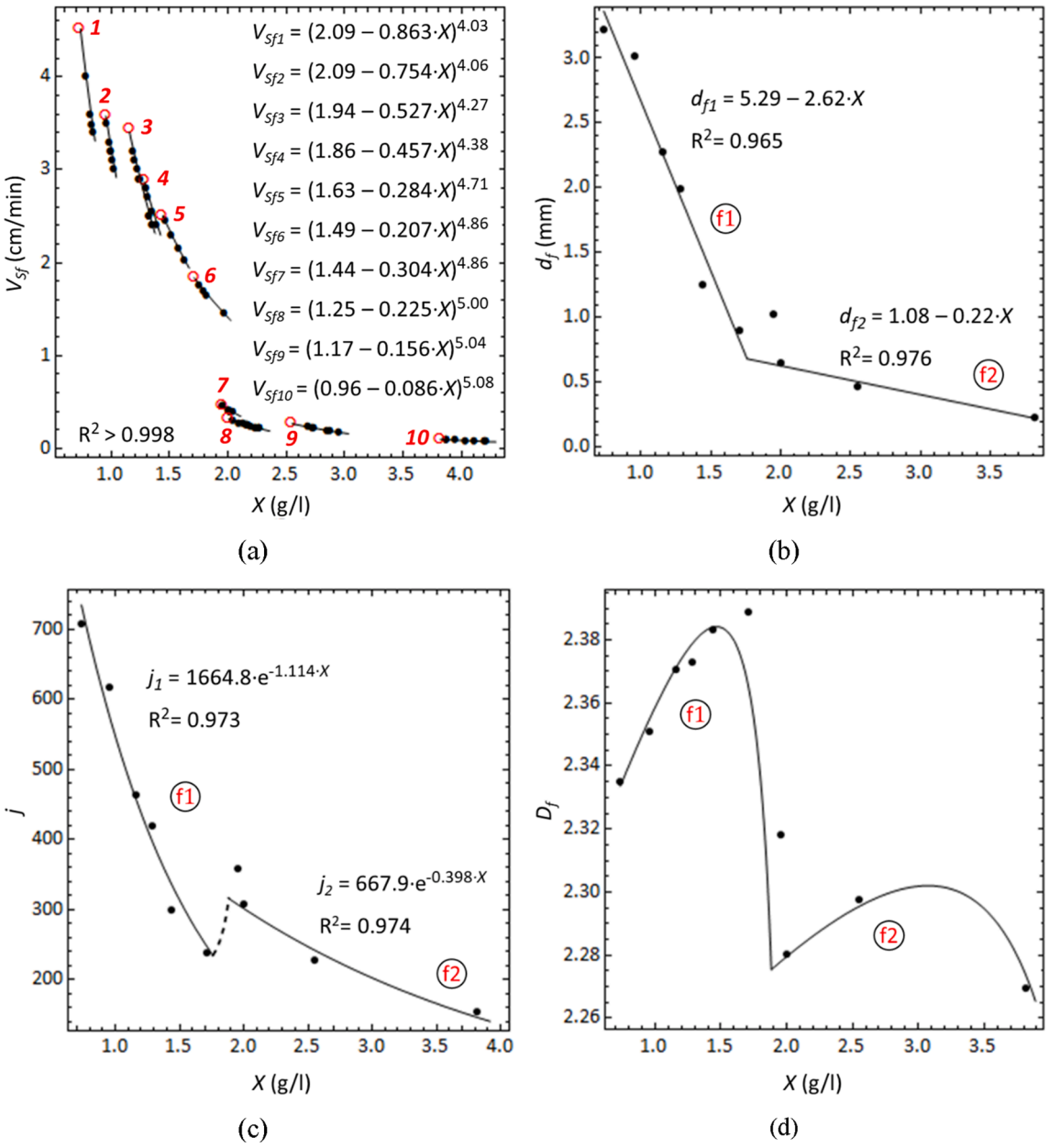

Fig. 6. (a) Final settling velocity obtained in the hindered settling zones (o) and in the transition zones (•) from the settling tests, together with the $V_{Sf}(X)$ regressions results using Eq. (6). $V_{Sf}(X)$ regressions results: (b) flocs equivalent diameters (d_f) with the $d_f(X)$ regression results, (c) aggregate volumetric index (j) with the $j(X)$ regression results and (d) flocs fractal dimension (D_f) with the model obtained for $D_f(X)$ by means of Eq. (11).

dimension allows establishing a link between zones f1 and f2.

$$D_f = 3 - \frac{ln\left(\frac{j_0 \cdot (\rho_p - \rho)}{\rho_s - \rho}\right) - k_j \cdot X}{ln\left(\frac{d_{f0} - k_f \cdot X}{d_p}\right)} \quad (11)$$

Introducing the fractal dimension into the model allows to eliminate the discontinuity in $j(X)$. Substituting Eq. (10a) and (11) into Eq. (5) leads to an expression that enables to describe the aggregate's volumetric index transition from zone f1 to zone f2, eliminating the discontinuity between both zones (discontinuous line in Fig. 6c). This relationship implies that if d_f changes smoothly when passing from zone f1 to zone f2 (Fig. 6b), the sharp decrease produced by the flocs fractal dimension causes the sudden increase of j.

Fig. 7a shows the flocs porosity due to the larger pores generated from the primary flocs (ε_{fp}) and Fig. 7b the relative increment in the average number of flocs per unit mass (n_f/X) with respect to the number of flocs per unit mass in the settling test with lower solids concentration (n_{f1}/X_1) as the ratio of n_f/X to n_{f1}/X_1 (rn_f/X). After the sludge acceleration process, the number of flocs increases, and the generated flocs porosity decreases with the increase of X. The decrease of j from increasing X implies that the volume of solids contained within the flocs increases per unit of flocs volume. This means a decrease in the water content inside the flocs, generating a decrease in flocs porosity and an increase in flocs density. Eqs. (7), (8), (10a) and (11) allow to calculate ε_{fp} and rn_f/X in each test and its variation with X. The evolution of the fractal dimension in the transition zone between zones f1 and f2 generates the abrupt variation in ε_{fp} and in rn_f/X (discontinuous line in Fig. 7a and b).

The values obtained from flocs porosity (ε_{fp}) are compatible with the experimental results collected in the bibliography. Li and Yuan [35] found that activated sludge had a fractal structure and that flocs porosity increased with flocs size between 0.87 and 0.98. Xiao et al. [39] studied

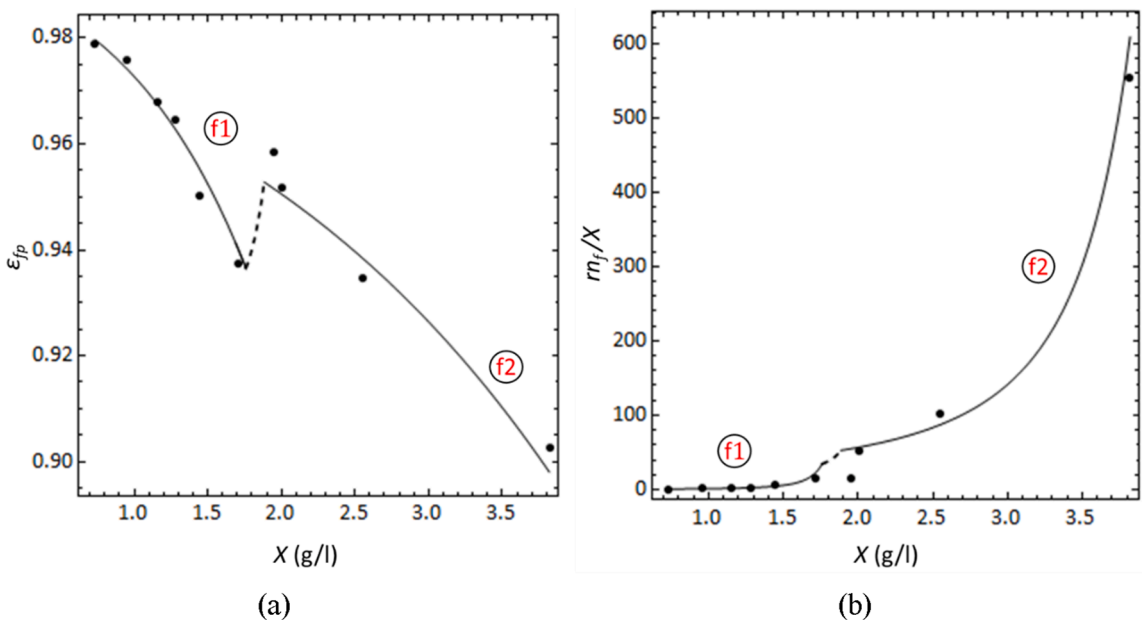

Fig. 7. (a) Flocs porosity (ε_{fp}) together with ε_{fp} (X) obtained from the model. (b) Ratio of average number of flocs per unit mass (rn_f/X) together with the rn_f/X (X) obtained from the model.

the flow of water through the activated sludge flocs after a flocculation process and obtained that these flocs porosities were between 0.91 and 0.98.

Considering all the results obtained, the characteristics of those flocs generated after the sludge acceleration process depend on X. An increase of X causes the number of flocs to increase, generating smaller, denser and with less porosity flocs. The sharp decrease in fractal dimension allows describing the abrupt variation of the rest of flocs properties.

3.4.2. Final hindered settling velocity model

The empirical description of the flocs characteristics after the sludge fragmentation and flocculation process, allows to study the effect of the change in the flocs structure on the final hindered settling velocity (V_{Sf}). Fig. 8a shows the experimental V_{Sf} values obtained in the constant final settling velocity zone (Fig. 3b), together with V_{Sf} (X) calculated by combination of Eqs. (6), (10a) and (11) (continuous line). The model was not adjusted by making a regression with the V_{Sf} experimental data, it was obtained from the regression made on d_f (X) and D_f(X).

The model allows to describe the abrupt decrease of settling velocity in the transition region between zones f1 and f2 from the experimental results of the settling tests in zone f1, where the decrease is not experimentally observed (Fig. 3b). It is important to note that the model parameters (Eq. (10)) were obtained using experimental data different from that used to determine the V_{Sf} values described by the model. The model parameters were obtained in the transition zones and the V_{Sf} values in the hindered settling zones, of the settling tests.

As observed in Fig. 9, which shows the V_{Sf} model predictions versus their experimental values, the proposed model correctly describes the final hindered settling velocity, since the slope of the regression line is very close to one (1.008) and the R^2 value is very high (0.984).

Fig. 8b shows the flocs terminal settling velocity obtained from the model fit in each settling test (Fig. 6a) and V_0(X) calculated with Eq. (6c), (6d), (10a) and (11) (continuous line). It can be observed that V_0 decreases rapidly in zone f1. The decrease of V_0, together with the sudden decrease of D_f at the transition between zone f1 and zone f2, causes a sharp decrease of the sludge final settling velocity. The V_0 values have the same order of magnitude than those obtained experimentally in other studies. Hriberšek et al. [40] obtained an activated sludge terminal settling velocity between 0.2 and 2.1 mm/s for flocs with a diameter from 0.15 to 1.7 mm, while Li and Yuan [35] obtained a velocity between 1.7 and 4.2 mm/s for flocs with a diameter from 1.3 to 2.4 mm.

Richardson and Zaki model is frequently used considering the Stokes law to calculate the flocs terminal settling velocity and fixing $n = 4.65$ [10–14], but this simplification is only valid for $Re < 0.2$ [8,9]. Fig. 8c shows that the variation of Reynolds number (Re) with X is approximately linear in zones f1 and f2 (Fig. 8c) and that the Re value is much larger than 0.2 in zone f1. The results obtained confirm the need to correct V_0 and calculate the exponent n as a function of Re since $Re < 0.2$ only in zone f2.

The model exponent (n) increases from 4.0 to 5.0 by increasing X in zone f1 (Fig. 8d) due to the decrease in Reynolds number. Since the model exponent obtained in the V_{Sf} fitting given in Fig. 3b is close to 5, V_{Sf} was calculated simplifying the model by setting $n = 5.0$ and eliminating the correction by Re in V_0. As shown in Fig. 8a (discontinuous line), this simplification is not valid in zone f1, so it is necessary to calculate n and V_0 as a function of Re to correctly describe V_{Sf} (X). This is also the case when the value $n = 4.65$ is set in the model.

The results obtained prove the validity of the proposed model for the activated sludge hindered settling velocity as a function of the fractal dimension and other flocs characteristics (Eq. (6)). Although in this study an empirical relation of d_f and j as a function of X was used, the model raises the possibility for future studies of combining the settling model with a flocculation model in order to describe the changes in the flocs characteristics during sludge acceleration process.

3.5. Description of the sludge fragmentation and flocculation stage

The following stages can be distinguished in sedimentation tests (Fig. 10): initial agitation of the sludge to reproduce WWTP conditions, induction stage where the initial sludge structure is formed from the primary flocs, initial stage with constant hindered settling velocity (V_{Si}), sludge acceleration where sludge fragmentation occurs as well as flocculation of the generated fragments causing a new floc structure, and final stage with constant hindered settling velocity (V_{Sf}).

The activated sludge flocs from the Ford WWTP are weak and easily breakable with a low turbulence due to their pin-point floc structure. The weak flocs breakage in the biological reactor due to the high turbulence produced by the mechanical aerators generates the primary flocs that then aggregate to form larger flocs in the secondary settling

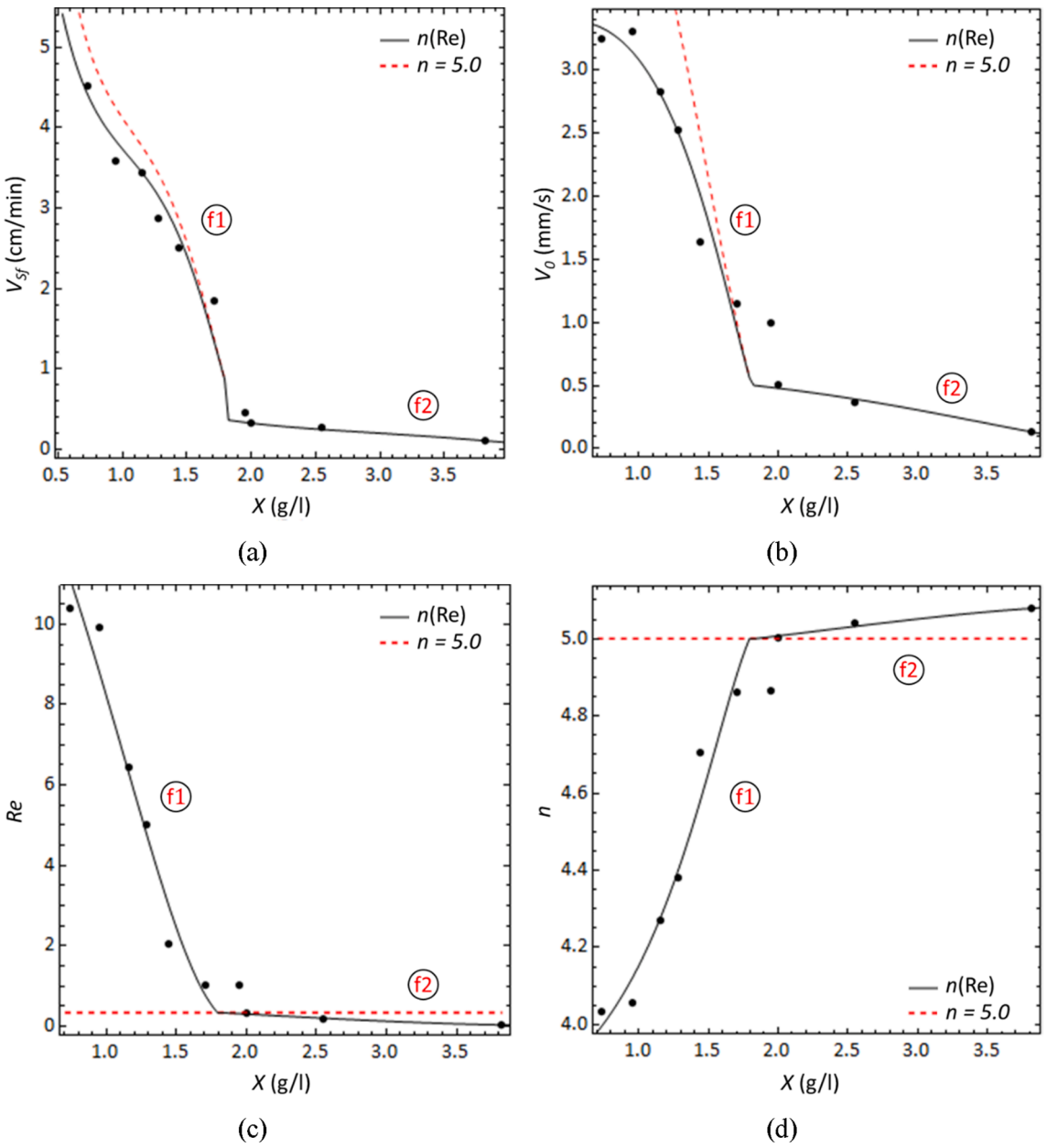

Fig. 8. (a) Final hindered settling velocity (V_{Sf}). (b) Flocs terminal settling velocity (V_0). (c) Reynolds number (Re). (d) Model exponent (n) for $V_{Sf}(X)$.

tank. The initial rapid sludge agitation in the settling tests enables to reproduce the described conditions in the biological treatment.

At the end of the initial agitation process in the settling tests, a short induction period was observed prior to the initial constant settling velocity stage (Fig. 10). During this period, a flocculation process takes place due to the combined effect of the turbulence dissipation and the beginning of the sludge sedimentation. The presence of Fe and Al salts, and polymers from the primary treatment allows the flocs in the described flocculation processes to aggregate easily making larger flocs from the primary ones.

In a previous study, Asensi et al. [15] described how after the induction stage a sludge structure formed by large flocs in zone i1 (Fig. 3b), for low X concentrations, or a weak gel structure in zone i2 (Fig. 3b), for high X concentrations, can be generated. The authors proposed an equation to calculate the concentration X_t (Fig. 3b) where the transition between zones i1 and i2 (or equivalently between zones f1 and f2) occurs by comparing the external porosity of the flocs formed in the induction stage with the internal porosity of the flocs due to the primary flocs. For $X < X_t$, where the external porosity is greater than the internal porosity, the sludge sedimentation and the formation of larger flocs is determined by the flow of water out of the flocs. While for $X > X_t$, where the external porosity is the same order as the internal porosity, the water flow inside the flocs plays an important role in floc formation. In this case, the distance between the formed flocs and the size of their pores is of the same order, thus, in the induction stage, a large amount of bonding between flocs occurs, giving rise to a weak gel-like structure.

At the end of the induction stage, an equilibrium is reached in the sludge structure and the stage with constant initial hindered settling velocity (V_{Si}) in zones i1 and i2 begins (Figs. 3 and 10).

After the initial stage with constant V_{Si}, a stage where the sludge is accelerated begins (Figs. 3 and 10). Asensi et al. [15] also studied the instant at which sludge acceleration (t_d) begins. They observed that the smaller the initial hindered settling velocity (V_{Si}) the greater t_d was, and that the t_d value depended on the presence of coagulants in the supernatant. They described the existence of physical and chemical mechanisms that trigger the fragmentation of the initial sludge structure and

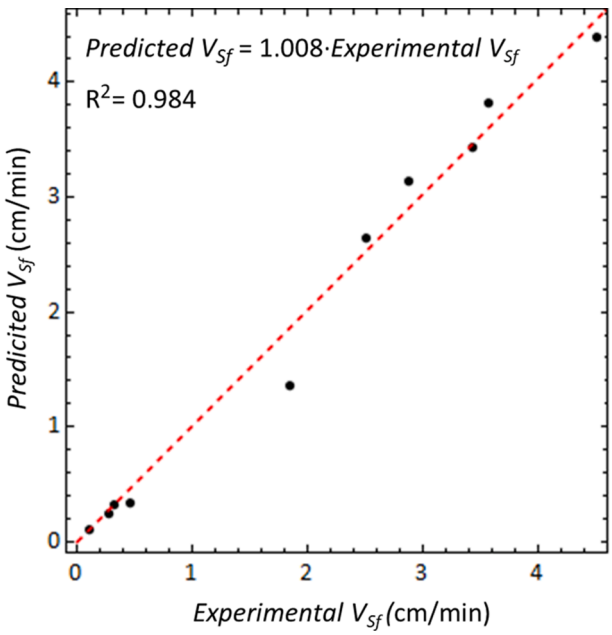

Fig. 9. Predicted final hindered settling velocity (V_{Sf}) versus experimental V_{Sf} values.

the subsequent flocculation process. For low X concentrations (zone i1) where V_{Si} is high, a physical fragmentation mechanism based on the existence of shear forces causing the breakage of bonds between the primary flocs predominates. In this case, fragmentation occurs at the points inside the floc where the pores are larger, generating large fragments of the flocs [15]. While for high X concentrations (zone i2) where V_{Si} is low, the chemical fragmentation mechanism predominates due to the instability of the bonds between the primary flocs. In this case, the fragmentation process is slower and more homogeneous, generating a larger number of small size flocs [15].

The fragmentation of an initial different sludge structure (large size flocs in zone i1 or weak gel in zone i2) and the change from a predominant physical mechanism of fragmentation in zone i1 to a chemical mechanism in zone i2, leads to a different flocculation mechanism. This enables to justify the formation of flocs with different characteristics in zones f1 and f2, and the sharp descent in D_f. The final stage with constant hindered settling velocity starts when an equilibrium is reached in the floc structure, at the end of the sludge acceleration stage (Figs. 3 and 10).

As mentioned above, for high X concentrations ($X > X_t$), a great number of bonds between primary flocs are produced in the induction stage, generating a weak gel structure in the i2 zone. During this stage of floc formation, the number of bonds between primary flocs increases with increasing X due to the larger number of flocs and the smaller distance between them. Subsequently, the predominance of the chemical fragmentation mechanism generates a slow and homogeneous breakage of the bonds between primary flocs in zone i2. Finally, gel fragmentation is triggered resulting in a great number of small fragments that aggregate and form a new floc structure in the sludge acceleration stage. The higher number of floc bonds that must be broken when X increases generates smaller and smaller fragments and causes the acceleration stage to be delayed (t_d increases exponentially with X). The flocculation process of smaller fragments can explain how increasing X produces a greater number of smaller, less porous, and more compact flocs in zone f2 (Figs. 6b, d, 7a and b).

The fractal dimension of the formed flocs depends on the breakage and existing aggregation mechanisms [41,42], and on the presence of metal salts and polyelectrolytes [19,22]. The physical and chemical fragmentation mechanisms described above will lead to a predominant breakage mode of large-scale fragmentation. However, floc breakage by surface erosion will be unimportant since these fragmentation mechanisms do not generate tangential forces that cause particle detachment from the floc surface. Thus, during the flocculation process originated during the sludge acceleration stage, the generated fragments will interact according to the cluster–cluster aggregation mechanism. Several theoretical studies have shown that the cluster–cluster aggregation mechanisms generate flocs with fractal dimensions between 1.78 and 2.09, while the particle-cluster aggregation mechanisms generate fractal dimensions between 2.5 and 3 [42]. These theoretical fractal dimensions constitute the fractal dimensions minimum value for flocs generated by these ideal mechanisms since they do not consider several factors such as the presence of coagulants. The fractal dimensions obtained in the settling tests are compatible with the fragmentation and flocculation mechanisms described above.

The $V_S(X)$ model proposed in this paper allows to consider future studies to link a model describing the discussed fragmentation and flocculation processes with the sludge final hindered settling velocity. The $V_S(X)$ model allows describing the abrupt decrease of the final hindered settling velocity, but it cannot explain the appearance of large size flocs in some of the tests in zone f1. On the other hand, considering the water flow through the flocs has allowed determining the

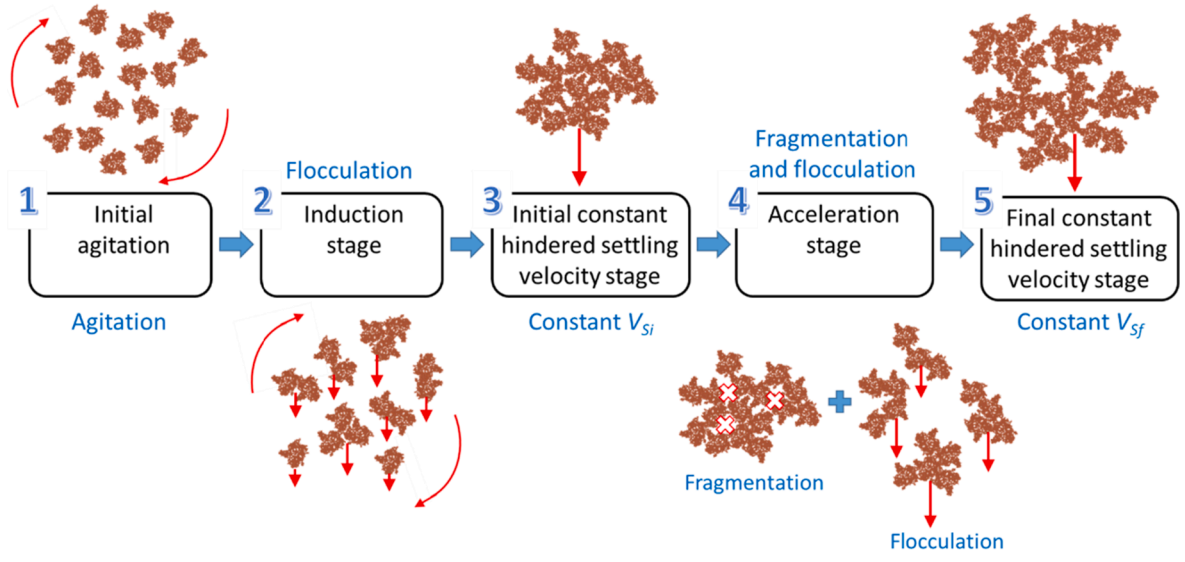

Fig. 10. Sequence of stages taking place in the sedimentation tests.

concentration X_t where the abrupt decrease of $V_S(X)$ occurs, as well as describing the physical mechanism of sludge fragmentation. The proposed model introduces the fractal structure and other physical characteristics of flocs, but it has the limitation of assuming that the flocs are spherical and impermeable. Therefore, it would be necessary in a future development to introduce into the model the sphericity of flocs and the effect of water flow due to the internal flocs porosity. In this way, it was possible to study how the sphericity and permeability of flocs affect the hindered settling velocity and the calculation of floc size.

4. Conclusions

A modification of Richardson and Zaki model for the hindered settling velocity as a function of the fractal dimension and other flocs characteristics was proposed. The model opens the possibility of linking the hindered settling process to other processes that affect the flocs structure: seasonal changes in flocs or disruptions in the biological treatment, addition of coagulants or an inert compound to improve the sedimentability of the sludge, etc.

The methodology used to calculate the settling velocity in the transition zone of the activated sludge settling tests together with the settling velocity model allowed to estimate the flocs characteristics.

The model was used to describe the settling velocity after a flocculation process originated by the activated sludge fragmentation. The introduction of the fractal dimension allows to describe the observed abrupt decrease of hindered settling velocity and the structure of the flocs formed from the primary flocs during the sludge acceleration phase. This abrupt $V_S(X)$ descent cannot be described by the classical hindered settling velocity models.

Reynolds number plays an important role in the model because $Re > 0.2$ in the settling tests carried out with a low suspended solids concentration.

CRediT authorship contribution statement

E. Asensi: Conceptualization, Methodology, Software, Validation, Formal analysis, Investigation, Writing – original draft. **E. Alemany:** Conceptualization, Methodology, Software, Validation, Formal analysis, Investigation, Writing – review & editing.

Declaration of Competing Interest

The authors declare that they have no known competing financial interests or personal relationships that could have appeared to influence the work reported in this paper.

Data availability

Data will be made available on request.

Acknowledgements

This research did not receive any specific grant from funding agencies in the public, commercial, or not-for-profit sectors.

Appendix A. Supplementary material

Supplementary data to this article can be found online at https://doi.org/10.1016/j.seppur.2022.121812.

References

[1] B. Li, M.K. Stenstrom, Research advances and challenges in one-dimensional modeling of secondary settling tanks – a critical review, Water Res. 65 (2014) 40–63, https://doi.org/10.1016/j.watres.2014.07.007.
[2] E. Torfs, S. Balemans, F. Locatelli, S. Diehl, R. Bürger, J. Laurent, P. François, I. Nopens, On constitutive functions for hindered settling velocity in 1-D settler models: Selection of appropriate model structure, Water Res. 110 (2017) 38–47, https://doi.org/10.1016/j.watres.2016.11.067.
[3] I. Takács, G.G. Patry, D. Nolasco, A dynamic model of the clarification-thickening process, Water Res. 25 (1991) 1263–1271, https://doi.org/10.1016/0043-1354(91)90066-Y.
[4] S.H. Cho, F. Colin, M. Sardin, C. Prost, Settling velocity model of activated sludge, Water Res. 27 (1993) 1237–1242, https://doi.org/10.1016/0043-1354(93)90016-B.
[5] E. Ramin, D.S. Wágner, L. Yde, P.J. Binning, M.R. Rasmussen, P.S. Mikkelsen, B. G. Plósz, A new settling velocity model to describe secondary sedimentation, Water Res. 66 (2014) 447–458, https://doi.org/10.1016/j.watres.2014.08.034.
[6] B.G. Plósz, J. Climent, C.T. Griffin, S. Chiva, R. Mukherjee, E. Penkarski-Rodon, M. Clarke, B. Valverde-Pérez, Hindered and compression solid settling functions – sensor data collection, practical model identification and validation, Water Res. 184 (2020) 116129.
[7] D.J. Kinnear, Biological Solids Sedimentation: A Model Incorporating Fundamental Settling Parameters, University of Utah, 2002. Ph.D. thesis.
[8] J.F. Richardson, W.N. Zaki, Sedimentation and fluidisation: Part I, Trans. Inst. Chem. Eng. 32 (1954) 35–53, https://doi.org/10.1016/S0263-8762(97)80006-8.
[9] R. Font, P. García, M. Rodriguez, Sedimentation test of metal hydroxides: hydrodynamics and influence of pH, Colloids Surf., A 157 (1999) 73–84, https://doi.org/10.1016/S0927-7757(99)00091-6.
[10] A.F. Grabsch, P.D. Fawell, S.J. Adkins, A. Beveridge, The impact of achieving a higher aggregate density on polymer-bridging flocculation, Int. J. Miner. Process. 124 (2013) 83–94, https://doi.org/10.1016/j.minpro.2013.04.011.
[11] A.R. Heath, P.A. Bahri, P.D. Fawell, J.B. Farrow, Polymer flocculation of calcite: relating the aggregate size to the settling rate, AIChE J. 52 (2006) 1987–1994, https://doi.org/10.1002/aic.10789.
[12] A.P.G. Lockwood, J. Peakall, N.J. Warren, G. Randall, M. Barnes, D. Harbottle, T. N. Hunter, Structure and sedimentation characterisation of sheared Mg(OH)2 suspensions flocculated with anionic polymers, Chem. Eng. Sci. 231 (2021) 116274.
[13] G.W. Chen, I.L. Chang, W.T. Hung, D.J. Lee, Regimes for zone settling of waste activated sludges, Water Res. 30 (1996) 1844–1850, https://doi.org/10.1016/0043-1354(95)00322-3.
[14] E. Asensi, E. Alemany, P. Duque-Sarango, D. Aguado, Assessment and modelling of the effect of precipitated ferric chloride addition on the activated sludge settling properties, Chem. Eng. Res. Des. 150 (2019) 14–25, https://doi.org/10.1016/j.cherd.2019.07.018.
[15] E. Asensi, E. Alemany, A. Seco, J. Ferrer, Characterization of activated sludge settling properties with a sludge collapse-acceleration stage, Sep. Purif. Technol. 209 (2019) 32–41, https://doi.org/10.1016/J.SEPPUR.2018.07.006.
[16] B. Jin, B.M. Wilén, P. Lant, A comprehensive insight into floc characteristics and their impact on compressibility and settleability of activated sludge, Chem. Eng. J. 95 (2003) 221–234, https://doi.org/10.1016/S1385-8947(03)00108-6.
[17] A.J. Schuler, H. Jang, Density effects on activated sludge zone settling velocities, Water Res. 41 (2007) 1814–1822, https://doi.org/10.1016/j.watres.2007.01.011.
[18] J. Yu, R. Zhao, Y. Gao, Y. Kim, Effects of particle size on the zone settling velocity of activated sludge, Environ. Eng. Sci. 33 (2016) 423–429, https://doi.org/10.1089/ees.2013.0509.
[19] E. Asensi, D. Zambrano, E. Alemany, D. Aguado, Effect of the addition of precipitated ferric chloride on the morphology and settling characteristics of activated sludge flocs, Sep. Purif. Technol. 227 (2019) 115711, https://doi.org/10.1016/J.SEPPUR.2019.115711.
[20] P.A. Jones, A.J. Schuler, Seasonal variability of biomass density and activated sludge settleability in full-scale wastewater treatment systems, Chem. Eng. J. 164 (2010) 16–22, https://doi.org/10.1016/j.cej.2010.07.061.
[21] E. Koivuranta, T. Suopajärvi, J. Hattuniemi, T. Stoor, M. Illikainen, The effect of seasonal variations on floc morphology in the activated sludge process, Environ. Technol. (U.K.) 38 (2017) 3209–3215, https://doi.org/10.1080/09593330.2017.1291760.
[22] Q. Chen, Y. Wang, Influence of single- and dual-flocculant conditioning on the geometric morphology and internal structure of activated sludge, Powder Technol. 270 (2015) 1–9, https://doi.org/10.1016/j.powtec.2014.10.002.
[23] Y.Q. Zhao, Settling behaviour of polymer flocculated water-treatment sludge. I: Analyses of settling curves, Sep. Purif. Technol. 35 (2004) 71–80, https://doi.org/10.1016/S1383-5866(03)00132-1.
[24] L.J. Teece, J.M. Hart, K.Y. Ni Hsu, S. Gilligan, M.A. Faers, P. Bartlett, Gels under stress: the origins of delayed collapse, Colloids Surf., A 458 (2014) 126–133, https://doi.org/10.1016/j.colsurfa.2014.03.018.
[25] R.B. Baird, A.D. Eaton, E.W. Rice, L. Bridgewater, American Public Health Association, A.W.W. Association, W.E. Federation, Standard Methods for the Examination of Water and Wastewater, 23rd ed.,, American Public Health Association, Washington DC, 2017.
[26] M.C. van Loosdrecht, P.H. Nielsen, D. Lopez-Vazquez, C.M. Brdjanovic, Experimental Methods in Wastewater Treatment, IWA Publishing, London, 2016.
[27] R. Bürger, J. Careaga, S. Diehl, A review of flux identification methods for models of sedimentation, Water Sci. Technol. 81 (2020) 1715–1722, https://doi.org/10.2166/wst.2020.113.
[28] D.R. Lester, S.P. Usher, P.J. Scales, Estimation of the hindered settling function R (φ) from batch-settling tests, AIChE J. 51 (2005) 1158–1168, https://doi.org/10.1002/aic.10333.
[29] S. Diehl, Estimation of the batch-settling flux function for an ideal suspension from only two experiments, Chem. Eng. Sci. 62 (2007) 4589–4601, https://doi.org/10.1016/J.CES.2007.05.025.

[30] F. Locatelli, P. François, J. Laurent, F. Lawniczak, M. Dufresne, J. Vazquez, K. Bekkour, Detailed velocity and concentration profiles measurement during activated sludge batch settling using an ultrasonic transducer, Separ. Sci. Technol. 50 (2015) 1059–1065, https://doi.org/10.1080/01496395.2014.980002.
[31] F. Betancourt, R. Bürger, S. Diehl, C. Mejías, Advanced methods of flux identification for clarifier-thickener simulation models, Miner. Eng. 63 (2014) 2–15, https://doi.org/10.1016/j.mineng.2013.09.012.
[32] I. Nopens, Modelling the activated sludge flocculation process: A population balance approach, 2005.
[33] H. Jang, A.J. Schuler, The case for variable density: a new perspective on activated sludge settling, Water Environ. Res. 79 (2007) 2298–2303, https://doi.org/10.2175/106143007X194347.
[34] M. Kuśnierz, Scale of small particle population in activated sludge flocs, Water Air Soil Pollut. 229 (2018) 327, https://doi.org/10.1007/s11270-018-3979-7.
[35] X.Y. Li, Y. Yuan, Settling velocities and permeabilities of microbial aggregates, Water Res. 36 (2002) 3110–3120, https://doi.org/10.1016/S0043-1354(01)00541-3.
[36] X.Y. Li, B.E. Logan, Permeability of fractal aggregates, Water Res. 35 (2001) 3373–3380, https://doi.org/10.1016/S0043-1354(01)00061-6.
[37] R.I. Jeldres, P.D. Fawell, B.J. Florio, Population balance modelling to describe the particle aggregation process: a review, Powder Technol. 326 (2018) 190–207, https://doi.org/10.1016/j.powtec.2017.12.033.
[38] A. Khelifa, P.S. Hill, Models for effective density and settling velocity of flocs, J. Hydraul. Res. 44 (2006) 390–401, https://doi.org/10.1080/00221686.2006.9521690.
[39] F. Xiao, K.M. Lam, X.Y. Li, Investigation and visualization of internal flow through particle aggregates and microbial flocs using particle image velocimetry, J. Colloid Interface Sci. 397 (2013) 163–168, https://doi.org/10.1016/j.jcis.2013.01.053.
[40] M. Hriberšek, B. Žajdela, A. Hribernik, M. Zadravec, Experimental and numerical investigations of sedimentation of porous wastewater sludge flocs, Water Res. 45 (2011) 1729–1735, https://doi.org/10.1016/j.watres.2010.11.019.
[41] A. Vahedi, B. Gorczyca, Predicting the settling velocity of flocs formed in water treatment using multiple fractal dimensions, Water Res. 46 (2012) 4188–4194, https://doi.org/10.1016/j.watres.2012.04.031.
[42] P. Meakin, Historical introduction to computer models for fractal aggregates, J. Sol-Gel Sci. Technol. 15 (1999) 97–117, https://doi.org/10.1023/A:1008731904082.